ISSN 1674-1056
http://cpb.iphy.ac.cn
http://iopscience.iop.org/cpb
中国物理 B
Chinese Physics
中国物理
Chinese Physics B

Chaotic analysis of Atangana-Baleanu derivative fractional order Willis aneurysm system

Fei Gao(高飞), Wen-Qin Li(李文琴), Heng-Qing Tong(童恒庆), Xi-Ling Li(李喜玲)
Citation: Chin. Phys. B . 2019, 28(9): 090501 . **doi:** 10.1088/1674-1056/28/090501
Journal homepage: http://cpb.iphy.ac.cn; http://iopscience.iop.org/cpb

What follows is a list of articles you may be interested in

Intrinsic fluctuation and susceptibility in somatic cell reprogramming process

Jian Shen(沈健), Xiaomin Zhang(张小敏), Qiliang Li(李齐亮), Xinyu Wang(王歆宇), Yunjie Zhao(赵蕴杰), Ya Jia(贾亚)
Chin. Phys. B . 2019, 28(4): 040503 . **doi:** 10.1088/1674-1056/28/4/040503

Parrondo's paradox for chaos control and anticontrol of fractional-order systems

Marius-F Danca and Wallace K S Tang
Chin. Phys. B . 2016, 25(1): 010505 . **doi:** 10.1088/1674-1056/25/1/010505

Control of fractional chaotic and hyperchaotic systems based on a fractional order controller

Li Tian-Zeng, Wang Yu, Luo Mao-Kang
Chin. Phys. B . 2014, 23(8): 080501 . **doi:** 10.1088/1674-1056/23/8/080501

Complex dynamical behavior and chaos control for fractional-order Lorenz-like system

Li Rui-Hong, Chen Wei-Sheng
Chin. Phys. B . 2013, 22(4): 040503 . **doi:** 10.1088/1674-1056/22/4/040503

Chaos detection and control in a typical power system

Hossein Gholizadeh, Amir Hassannia, Azita Azarfar
Chin. Phys. B . 2013, 22(1): 010503 . **doi:** 10.1088/1674-1056/22/1/010503

Chaotic analysis of Atangana–Baleanu derivative fractional order Willis aneurysm system*

Fei Gao(高飞)†, Wen-Qin Li(李文琴), Heng-Qing Tong(童恒庆), and Xi-Ling Li(李喜玲)

School of Science, Wuhan University of Technology, Wuhan 430070, *China*

(Received 23 April 2019; revised manuscript received 14 June 2019; published online 30 August 2019)

A new Willis aneurysm system is proposed, which contains the Atangana–Baleanu(AB) fractional derivative. we obtain the numerical solution of the Atangana–Baleanu fractional Willis aneurysm system (ABWAS) with the AB fractional integral and the predictor–corrector scheme. Moreover, we research the chaotic properties of ABWAS with phase diagrams and Poincare sections. The different values of pulse pressure and system order are used to evaluate and compare their effects on ABWAS. The simulations verify that the changes of pulse pressure and system order are the significant reason for ABWAS' states varying from chaotic to steady. In addition, compared with Caputo fractional WAS (FWAS), ABWAS shows less state that is chaotic. Furthermore, the results of bifurcation diagrams of blood flow damping coefficient and reciprocal heart rate show that the blood flow velocity tends to stabilize with the increase of blood flow damping coefficient or reciprocal heart rate, which is consistent with embolization therapy and drug therapy for clinical treatment of cerebral aneurysms. Finally, in view of the fact that ABWAS in chaotic state increases the possibility of rupture of cerebral aneurysms, a reasonable controller is designed to control ABWAS based on the stability theory. Compared with the control results of FWAS by the same method, the results show that the blood flow velocity in the ABWAS system varies in a smaller range. Therefore, the control effect of ABWAS is better and more stable. The new Willis aneurysm system with Atangana–Baleanu fractional derivative provides new information for the further study on treatment and control of brain aneurysms.

Keywords: fractional Willis aneurysm system, Atangana–Baleanu fractional differential, Poincaré section, chaos control

PACS: 05.45.–a, 05.45.Gg, 05.45.Pq **DOI:** 10.1088/1674-1056/ab38a4

1. Introduction

The dynamic behaviors of chaotic systems have received increasing attention in recent decades. Some research revolved around the dynamic behavior of the models. In Ref. [1], a new model that can reduce the chaotic region was obtained by introducing a new variable. Wang *et al.*[2] proposed a pseudo-random coupling method which can accelerate the chaotic behavior of the full space. In Ref. [3], the complex dynamics of a geomagnetic field system were explored by introducing a non-smooth factor. The Willis aneurysm system is a biomedical chaotic system that has attracted researchers' interest in recent years. Cerebral aneurysms are prone to rupture, which leads to high disability and mortality,[4] and the circle of Willis is a high incidence area of cerebral aneurysms. Therefore, it is necessary to predict and control the formation and growth of cerebral aneurysms by analyzing the chaotic dynamics of the Willis aneurysms system. The research on the Wills aneurysm system can be divided into the following three aspects: periodic solution, control method, and fractional order system.

In Ref. [5], Austin explained that a physical circuit can be used to simulate the flow of blood in a brain aneurysm, and a biomechanical model of Willis cerebral aneurysm was presented. This model reveals the non-linear relationship between the volumes and the pressure in the cerebral aneurysm. Some information to prevent rupture and swelling of the cerebral aneurysm was presented. However, the Austin model has limitations due to the omission of damping and certain constraints. Therefore, in Refs. [6] an [7], a Duffing equation with damping terms and forced external excitation was obtained by reanalyzing the analog circuit of Austin. Some studies were based on this new equation. Cao *et al.*[8] proved that the equation has at least one periodic solution under certain conditions. The condition of Devaney chaos in the Willis brain aneurysm model was obtained by the method of Melnikov function in Ref. [9]. The condition for the existence of the periodic solution of the system was obtained by Feng.[10] Nieto *et al.*[11] considered the existence of the solution of the periodic boundary value problem for the Willis aneurysm system.

The chaotic state of the Willis aneurysm system is harmful and chaos should be avoided as much as possible. In view of this problem, some scholars have discussed the control of the Willis aneurysm system. For the variable parameter Willis aneurysm system, based on the adaptive control idea, synchronization of two parameters of the Willis aneurysm system was obtained through the construction parameter adaptive

*Project supported by the State Key Program of the National Natural Science of China (Grant No. 91324201), the Fundamental Research Funds for the Central Universities of China, the Self–determined and Innovative Research Funds of WUT, China (Grant No. 2018IB017), and the Natural Science Foundation of Hubei Province of China (Grant No. 2014CFB865).

†Corresponding author. E-mail: hgaofei@gmail.com

© 2019 Chinese Physical Society and IOP Publishing Ltd

law in Ref. [12] . Aiming at the control problem of the Willis aneurysm system with uncertainty, Peng *et al.*[13] proposed an adaptive fuzzy sliding mode control method. Sun *et al.*[14] studied a new Willis ring brain aneurysm mathematical model by introducing the antihypertensive drug excitation term function. The control method of antihypertensive drugs was presented.

All the above literatures only focussed on the integer-order Willis aneurysm system. Considering that the integer-order Willis aneurysm system has certain defects in describing the complex dynamics of blood flow, Cao *et al.*[15] studied a fractional order Willis aneurysm system based on Caputo derivative. This system was effectively controlled by the method of designing a controller and the drug excitation term function.

Many researches have analyzed the merits and drawbacks of fractional derivatives and put forward different definitions. Riemann–Liouville fractional derivative and Caputo fractional derivative are based on the power law functions. These two fractional derivatives have been in practice for a long time and applied to various practical problems successfully.[16,17] However, their kernel has a singularity, the kernel of Caputo derivative is a singular and the derivative of a constant is not zero in case of Riemann–Liouville fractional derivative.[18,19] Therefore, Caputo and Fabrizio[18] presented a new definition having non-singularity in the kernel to overcome the problem in 2015. Some research[20,21] revolved around the Caputo–Fabrizio fractional derivative. Besides the definition of Caputo–Fabrizio fractional derivative, Atangana and Baleanu[22] presented a new fractional definition in 2016. The Atangana–Baleanu (AB) fractional-order derivative is known to possess nonsingularity as well as nonlocality of the kernel, which adopts the generalized Mittag–Leffler function. The AB fractional derivative has all the benefits of the above fractional derivatives.[23] Recently, the Atangana–Baleanu fractional derivative has been applied in many fields, for instance, in biology and ecology,[24,25] electrical circuit,[26–28] fluid model,[29–32] groundwater,[33,34] and chaos theory[35,36] among many others.

Firstly, blood as a viscoelastic body[37] in soft matter[38] has the fluid viscosity and the elasticity of solids. Thus it has a complex flow pattern. Besides, the vascular system is a relatively complicated elastic piping system. Secondly, the brain aneurysm is a swelling area in the cerebral artery wall, and the system of Willis aneurysm involves the state and nature of the blood and vascular system. Therefore, the Willis aneurysm system has a complex dynamic mechanism. Finally, the asymptotic behavior of AB derivative makes it more advantageous than simple Caputo derivative in simulating complex phenomena.[39] The fractional order Willis aneurysm system with AB derivative has not considered before. Therefore, on the basis of the above three points, we consider a fractional order Willis aneurysm system using the new AB fractional derivative.

The main structure of this paper is as follows. The basic definitions of AB derivative are presented in Section 2. In Section 3, the Atangana–Baleanu fractional Willis aneurysm system (ABWAS) is created and the simulation results show that the ABWAS system has the chaotic phenomenon. In addition, we compare the effects of system order and pulse pressure on ABWAS and Caputo fractional WAS (FWAS). The effects of blood flow damping coefficient and reciprocal heart rate on the ABWAS are also given. In Section 4, the control of ABWAS is studied by the method of designing a reasonable controller through stability conditions. Furthermore, we compare the control effect for ABWAS and FWAS. Finally, this article is concluded in Section 5.

2. Preliminaries

The definitions of the Atangana–Baleanu fractional derivative and integral are shown in this section. Besides, we have the conclusion that the AB fractional Willis aneurysm system with initial conditions is stable.

Definition 1[22] For $\alpha \in [0,1]$, $f \in H^1(x,y)$, $y > x$, with the function f differentiable, the definition of the new fractional derivative (Atangana–Baleanu derivative in Caputo sense) is given as

$$ {}^{\mathrm{AB}}_{l}D^{\alpha}_{t}[f(t)] = \frac{B(\alpha)}{1-\alpha}\int_{l}^{t}\frac{\mathrm{d}}{\mathrm{d}\,j}[g(j)]E_{\alpha}\left[-\frac{\alpha(t-j)^{\alpha}}{1-\alpha}\right]\mathrm{d}\,j, \quad (1) $$

where B satisfies the following $B(0)=B(1)=1$, and $E_{\alpha}(t^{\alpha}) = \sum_{v=0}^{\infty}\frac{t^{\alpha v}}{\Gamma(\alpha v+1)}$.

Definition 2[22] The fractional integral associate to the new fractional derivative with nonlocal kernel (Atangana–Baleanu fractional integral) is defined as

$$ {}^{\mathrm{AB}}_{b}I^{\alpha}_{t}[f(t)] = \frac{1-\alpha}{B(\alpha)}f(t) + \frac{\alpha}{B(\alpha)\Gamma(\alpha)}\int_{b}^{t}f(s)(t-s)^{\alpha-1}\mathrm{d}s. \quad (2) $$

Theorem 1 The AB fractional system with initial conditions is as follow:

$$ \begin{cases} {}^{\mathrm{AB}}_{0}D^{\alpha}_{t}\boldsymbol{y} = \boldsymbol{V}(t,\boldsymbol{y}(t)), \\ \boldsymbol{y}(0) = \boldsymbol{m}, \end{cases} \quad (3) $$

where $\boldsymbol{V}(t,\boldsymbol{y}(t))$ satisfies the Lipschitz condition and $\boldsymbol{V}(t,0)$ is always zero. When the system order is in the interval $(0,1)$, for any state variable $\boldsymbol{y}(t) \in \mathbb{R}^n$, $\boldsymbol{m} \in \mathbb{R}^n$, the system (3) is stable under the conditions that we can find positive definite matrix $\boldsymbol{W}$ such that

$$ P(\boldsymbol{y}) = \boldsymbol{y}(t)^{\mathrm{T}}\boldsymbol{W}\,{}^{\mathrm{AB}}_{0}D^{\alpha}_{t}\boldsymbol{y}(t) \le 0. \quad (4) $$

Proof Let $0<\alpha<1$, according to the AB fractional integral, the solution of system (3) is shown as follow:

$$\boldsymbol{y}(t) = \boldsymbol{y}(0)+\frac{1-\alpha}{B(\alpha)}\boldsymbol{V}(t,\boldsymbol{y}(t)) + \frac{\alpha}{B(\alpha)\Gamma(\alpha)}\int_0^t \boldsymbol{V}(u,\boldsymbol{y}(u))(t-u)^{\alpha-1}\mathrm{d}u. \quad (5)$$

According to the definition of the derivative, we obtain

$$\begin{aligned}&\lim_{\Delta t\to 0}\frac{\boldsymbol{y}(t)-\boldsymbol{y}(t-\Delta t)}{\Delta t}\\ =&\lim_{\Delta t\to 0}\frac{\boldsymbol{y}(0)-\boldsymbol{y}(0)}{\Delta t}\\ &+\frac{1-\alpha}{B(\alpha)}\lim_{\Delta t\to 0}\frac{\boldsymbol{V}(t,\boldsymbol{y}(t))-\boldsymbol{V}(t-\Delta t,\boldsymbol{y}(t-\Delta t))}{\Delta t}\\ &+\frac{\alpha}{B(\alpha)\Gamma(\alpha)}\lim_{\Delta t\to 0}\frac{1}{\Delta t}\left[\int_0^t \boldsymbol{V}(u,\boldsymbol{y}(u))(t-u)^{\alpha-1}\mathrm{d}u\right.\\ &\left.-\int_0^{t-\Delta t}\boldsymbol{V}(u,\boldsymbol{y}(u))(t-u)^{\alpha-1}\mathrm{d}u\right]. \quad (6)\end{aligned}$$

The above equation is simplified as follow:

$$\begin{aligned}&\lim_{\Delta t\to 0}\frac{\boldsymbol{y}(t)-\boldsymbol{y}(t-\Delta t)}{\Delta t}\\ =&\lim_{\Delta t\to 0}\frac{\boldsymbol{y}(0)-\boldsymbol{y}(0)}{\Delta t}\\ &+\frac{1-\alpha}{B(\alpha)}\lim_{\Delta t\to 0}\frac{\boldsymbol{V}(t,\boldsymbol{y}(t))-\boldsymbol{V}(t-\Delta t,\boldsymbol{y}(t-\Delta t))}{\Delta t}\\ &+\frac{\alpha}{B(\alpha)\Gamma(\alpha)}\lim_{\Delta t\to 0}\frac{1}{\Delta t}\left[\int_{t-\Delta t}^t \boldsymbol{V}(u,\boldsymbol{y}(u))(t-u)^{\alpha-1}\mathrm{d}u\right]. \quad (7)\end{aligned}$$

Thus,

$$\mathrm{d}\boldsymbol{y}(t) = \frac{1-\alpha}{B(\alpha)}\lim_{\Delta t\to 0}\boldsymbol{V}(t,\boldsymbol{y}(t))-\boldsymbol{V}(t-\Delta t,\boldsymbol{y}(t-\Delta t))+\frac{\alpha}{B(\alpha)\Gamma(\alpha)}\lim_{\Delta t\to 0}\int_{t-\Delta t}^t \boldsymbol{V}(u,\boldsymbol{y}(u))(t-u)^{\alpha-1}\mathrm{d}u. \quad (8)$$

Constructing a positive definite function $G=\frac{1}{2}\boldsymbol{y}(t)^{\mathrm{T}}\boldsymbol{W}\boldsymbol{y}(t)$, we have

$$\begin{aligned}\mathrm{d}G=\boldsymbol{y}(t)^{\mathrm{T}}\boldsymbol{W}\mathrm{d}\boldsymbol{y}(t) =& \frac{1-\alpha}{B(\alpha)}\lim_{\Delta t\to 0}\boldsymbol{y}(t)^{\mathrm{T}}\boldsymbol{W}\boldsymbol{V}(t,\boldsymbol{y}(t))-\boldsymbol{y}(t)^{\mathrm{T}}\boldsymbol{W}\boldsymbol{V}(t-\Delta t,\boldsymbol{y}(t-\Delta t))\\ &+\frac{\alpha}{B(\alpha)\Gamma(\alpha)}\lim_{\Delta t\to 0}\int_{t-\Delta t}^t \boldsymbol{y}(t)^{\mathrm{T}}\boldsymbol{W}\boldsymbol{V}(u,\boldsymbol{y}(u))(t-u)^{\alpha-1}\mathrm{d}u. \quad (9)\end{aligned}$$

By using the assumptions of the theorem, the following formula can be derived:

$$P(\boldsymbol{y}(t))=\boldsymbol{y}(t)^{\mathrm{T}}\boldsymbol{W}\,{}_0^{\mathrm{AB}}D_t^{\alpha}\boldsymbol{y}(t)=\boldsymbol{y}(t)^{\mathrm{T}}\boldsymbol{W}\boldsymbol{V}(t,\boldsymbol{y}(t))\le 0, \quad (10)$$

$\boldsymbol{V}(t,y(t))$ satisfies the Lipschitz condition, therefore

$$|\boldsymbol{V}(t,\boldsymbol{y}(t))-\boldsymbol{V}(t-\Delta t,\boldsymbol{y}(t-\Delta t))|\le L|\boldsymbol{y}(t)-\boldsymbol{y}(t-\Delta t)|, \quad (11)$$

$$\begin{aligned}G'=\lim_{\Delta t\to 0}\frac{\Delta G}{\Delta t} =& \lim_{\Delta t\to 0}\frac{1-\alpha}{B(\alpha)}\lim_{\Delta t\to 0}\frac{\boldsymbol{y}(t)^{\mathrm{T}}\boldsymbol{W}\boldsymbol{V}(t,\boldsymbol{y}(t))-\boldsymbol{y}(t)^{\mathrm{T}}\boldsymbol{W}\boldsymbol{V}(t-\Delta t,\boldsymbol{y}(t-\Delta t))}{\Delta t}\\ &+\lim_{\Delta t\to 0}\frac{\alpha}{B(\alpha)\Gamma(\alpha)}\lim_{\Delta t\to 0}\frac{1}{\Delta t}\int_{t-\Delta t}^t \boldsymbol{y}(t)^{\mathrm{T}}\boldsymbol{W}\boldsymbol{V}(u,\boldsymbol{y}(u))(t-u)^{\alpha-1}\mathrm{d}u\le 0. \quad (12)\end{aligned}$$

According to the Lyapunov stability theory, $\lim_{t\to\infty}G=\frac{1}{2}\boldsymbol{y}(t)^{\mathrm{T}}\boldsymbol{W}\boldsymbol{y}(t)=0$. Therefore, $\lim_{t\to\infty}|\boldsymbol{y}(t)|=0$ and the system (3) is stable. This completes the proof.

3. Willis aneurysm system with Atangana–Baleanu derivative

3.1. Establishment of ABWAS

From Ref. [15], the Caputo fractional Willis aneurysm system is presented as follow:

$$\begin{cases}D_*^{q_1}x=y,\\ D_*^{q_2}y=F\cos(\omega t)-\mu y-\alpha x+\beta x^2-\gamma x^3,\\ 0<q_1,q_2<2,\end{cases} \quad (13)$$

where x denotes the blood flow velocity, y represents the blood flow change rate, F is the pulse pressure, μ stands for the damping coefficient of the blood flow, ω denotes the reciprocal of heart rate. The parameters α, β, and γ are related to the blood flow resistance and the elasticity of the vessel wall. These parameters are related to the human physiological structure and aneurysm status.

By changing the Caputo fractional differential of system (13) into the Atangana-Beleanu fractional differential, we obtain the ABWAS

$$\begin{cases}{}_0^{\mathrm{AB}}D_t^{q_1}x=y,\\ {}_0^{\mathrm{AB}}D_t^{q_2}y=F\cos(\omega t)-\mu y-\alpha x+\beta x^2-\gamma x^3,\\ 0<q_1,\ q_2<2.\end{cases} \quad (14)$$

3.2. Numerical approximations of ABWAS

For the sake of simplicity, equation (14) is rewritten as follow:

$$\begin{cases}{}_0^{\mathrm{AB}}D_t^{\alpha}x=y,\\ {}_0^{\mathrm{AB}}D_t^{\alpha}y=F\cos(\omega t)-\mu y-\alpha x+\beta x^2-\gamma x^3.\end{cases} \quad (15)$$

Applying the Atangana–Baleanu fractional integral to system (15), we obtain

$$\begin{aligned} x(t) &= x_0(t)+\frac{1-\alpha}{B(\alpha)}y+\frac{\alpha}{B(\alpha)\Gamma(\alpha)}\int_0^t y(t-\tau)^{\alpha-1}\,\mathrm{d}\tau,\\ y(t) &= y_0(t)+\frac{1-\alpha}{B(\alpha)}\left(F\cos(\omega t)-\mu y-\alpha x+\beta x^2-\gamma x^3\right)\\ &\quad+\frac{\alpha}{B(\alpha)\Gamma(\alpha)}\int_0^t\left(F\cos(\omega t)-\mu y-\alpha x+\beta x^2-\gamma x^3\right)\\ &\quad\times(t-\tau)^{\alpha-1}\,\mathrm{d}\tau. \end{aligned} \tag{16}$$

For the ABWAS system (15), by employing the prediction correction method,[40] the iterative formulas are derived as follows:

$$\begin{aligned} x_{n+1}(t) &= x_0(t)+\frac{1-\alpha}{B(\alpha)}y^p_{n+1}+\frac{\alpha}{B(\alpha)\Gamma(\alpha)}\left[\sum_{j=0}^{n}a_{1,j,n+1}y_j+a_{1,n+1,n+1}y^p_{n+1}\right],\\ y_{n+1}(t) &= y_0(t)+\frac{1-\alpha}{B(\alpha)}\left(F\cos(\omega t)-\mu y^p_{n+1}-\alpha x^p_{n+1}+\beta\left(x^p_{n+1}\right)^2-\gamma\left(x^p_{n+1}\right)^3\right)\\ &\quad+\frac{\alpha}{B(\alpha)\Gamma(\alpha)}\left[\sum_{j=0}^{n}a_{2,j,n+1}\left(F\cos(\omega t)-\mu y_j-\alpha x_j+\beta\left(x_j\right)^2-\gamma\left(x_j\right)^3\right)\right.\\ &\quad\left.+a_{2,n+1,n+1}\left(F\cos(\omega t)-\mu y^p_{n+1}-\alpha x^p_{n+1}+\beta\left(x^p_{n+1}\right)^2-\gamma\left(x^p_{n+1}\right)^3\right)\right], \end{aligned} \tag{17}$$

$$\begin{aligned} x^p_{n+1}(t) &= x_0(t)+\frac{1-\alpha}{B(\alpha)}y_n+\frac{\alpha}{B(\alpha)\Gamma(\alpha)}\sum_{j=0}^{n}b_{1,j,n+1}y_j,\\ y^p_{n+1}(t) &= y_0(t)+\frac{1-\alpha}{B(\alpha)}\left(F\cos(\omega t)-\mu y_n-\alpha x_n+\beta\left(x_n\right)^2-\gamma\left(x_n\right)^3\right)\\ &\quad+\frac{\alpha}{B(\alpha)\Gamma(\alpha)}\sum_{j=0}^{n}b_{2,j,n+1}\left(F\cos(\omega t)-\mu y_j-\alpha x_j+\beta\left(x_j\right)^2-\gamma\left(x_j\right)^3\right), \end{aligned} \tag{18}$$

$$a_{1,j,n+1}=a_{2,j,n+1}=\begin{cases}\dfrac{h^\alpha}{\alpha(\alpha+1)}\left[n^{\alpha+1}-(n-\alpha)(n+1)^\alpha\right], & j=0,\\ \dfrac{h^\alpha}{\alpha(\alpha+1)}\left[(n-j+2)^{\alpha+1}-2(n-j+1)^{\alpha+1}+(n-j)^{\alpha+1}\right], & 1\le j\le n,\\ \dfrac{h^\alpha}{\alpha(\alpha+1)}, & j=n+1.\end{cases} \tag{19}$$

$$b_{1,j,n+1}=b_{2,j,n+1}=\frac{h^\alpha}{\alpha}\left[(n-j+1)^\alpha-(n-j)^\alpha\right],\quad 0\le j\le n. \tag{20}$$

The iteration formulas can further be simplified as follows:

$$\begin{aligned} x^p_{n+1}(t) &= x_0(t)+\frac{1-\alpha}{B(\alpha)}y_n+\frac{h^\alpha}{B(\alpha)\Gamma(\alpha)}\sum_{j=0}^{n}b_{1,j,n+1}y_j,\\ y^p_{n+1}(t) &= y_0(t)+\frac{1-\alpha}{B(\alpha)}\left(F\cos(\omega t)-\mu y_n-\alpha x_n+\beta\left(x_n\right)^2-\gamma\left(x_n\right)^3\right)\\ &\quad+\frac{h^\alpha}{B(\alpha)\Gamma(\alpha)}\sum_{j=0}^{n}b_{2,j,n+1}\left(F\cos(\omega t)-\mu y_j-\alpha x_j+\beta\left(x_j\right)^2-\gamma\left(x_j\right)^3\right), \end{aligned} \tag{21}$$

$$b_{1,j,n+1}=b_{2,j,n+1}=\left[(n-j+1)^\alpha-(n-j)^\alpha\right],\quad 0\le j\le n, \tag{22}$$

$$\begin{aligned} x_{n+1}(t) &= x_0(t)+\frac{1-\alpha}{B(\alpha)}y^p_{n+1}+\frac{\alpha h^\alpha}{B(\alpha)\Gamma(\alpha+2)}\sum_{j=0}^{n}a_{1,j,n+1}y_j+\frac{\alpha h^\alpha}{B(\alpha)\Gamma(\alpha+2)}a_{1,n+1,n+1}y^p_{n+1},\\ y_{n+1}(t) &= y_0(t)+\frac{1-\alpha}{B(\alpha)}\left(F\cos(\omega t)-\mu y^p_{n+1}-\alpha x^p_{n+1}+\beta\left(x^p_{n+1}\right)^2-\gamma\left(x^p_{n+1}\right)^3\right)\\ &\quad+\frac{\alpha h^\alpha}{B(\alpha)\Gamma(\alpha+2)}\sum_{j=0}^{n}a_{2,j,n+1}\left(F\cos(\omega t)-\mu y_j-\alpha x_j+\beta\left(x_j\right)^2-\gamma\left(x_j\right)^3\right)\\ &\quad+\frac{\alpha h^\alpha}{B(\alpha)\Gamma(\alpha+2)}a_{2,n+1,n+1}\left(F\cos(\omega t)-\mu y^p_{n+1}-\alpha x^p_{n+1}+\beta\left(x^p_{n+1}\right)^2-\gamma\left(x^p_{n+1}\right)^3\right), \end{aligned} \tag{23}$$

$$a_{1,j,n+1}=a_{2,j,n+1}=\begin{cases}\left[n^{\alpha+1}-(n-\alpha)(n+1)^\alpha\right], & j=0,\\ \left[(n-j+2)^{\alpha+1}-2(n-j+1)^{\alpha+1}+(n-j)^{\alpha+1}\right], & 1\le j\le n,\\ 1, & j=n+1.\end{cases} \tag{24}$$

3.3. Comparison of results between FWAS and ABWAS

For system (14) and system (13), the parameters are taken as follows: $\alpha = 0.9$, $\beta = 3$, $\gamma = 2$, $F = 0.11$, $\mu = 0.1$, $\omega = 1$. If there are dense points and these points have a hierarchical structure on the Poincaré section, then it can be judged that the system is in a chaotic state. Figure shows the curves of x–t and y–t, time course, phase diagram, and Poincaré section of system (14) for $q_1 = 1.02$, $q_2 = 0.97$. As can be seen in the Poincaré section (Fig. 1(d)), system (14) exhibits complex chaos.

Since systems (13) and (14) are affected by many parameters, it is difficult to find the parameters that make the results of the two systems completely equal. However, when the parameters of system (14) are taken as follows: $q_1 = 1.02$, $q_2 = 0.97$, $\alpha = 0.9$, $\beta = 3$, $\gamma = 2$, $F = 0.11$, $\mu = 0.1$, $\omega = 1$; and the parameters of system (13) are taken as follows: $q_1 = 1.03$, $q_2 = 0.96$, $\alpha = 0.9$, $\beta = 3$, $\gamma = 2$, $F = 0.11$, $\mu = 0.1$, $\omega = 1$, we obtain approximately the same results of the two systems. Figure 2 shows the phase diagram and Poincaré section of the two systems when the parameters are set as above. From Fig. 2, it can be seen that the phase diagram and Poincaré section of systems (14) and (13) are basically coincident in shape and structure.

In order to compare the results of FWAS and ABWAS when $q_1 = 1$, $q_2 = 1$, we consider the cases with $F = 0.095$ (Figs. 3(a) and 3(d)), $F = 0.097$ (Figs. 3(b) and 3(e)), and $F = 0.1$ (Figs. 3(c) and 3(f)). In addition, other parameters are unchanged. The first three figures in Fig. 3 show the the phase diagram of FWAS when $q_1 = 1$, $q_2 = 1$. In the last three figures of Fig. 3, we present the phase diagram of ABWAS when $q_1 = 1$, $q_2 = 1$. The results of Fig. 3 show that the phase diagram structure is basically the same when the system order of ABWAS and FWAS is equal to 1. However, when the value

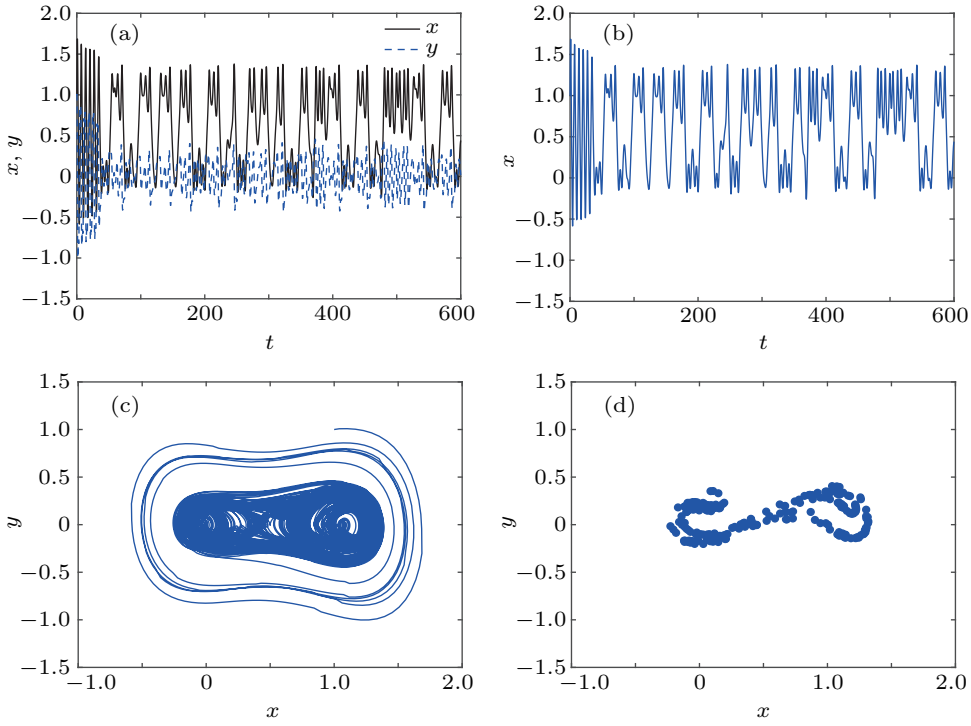


Fig. 1. System order of ABWAS in the case of $q_1 = 1.02$ and $q_2 = 0.97$: (a) x–t and y–t curves, (b) time course, (c) phase diagram, (d) Poincaré section.

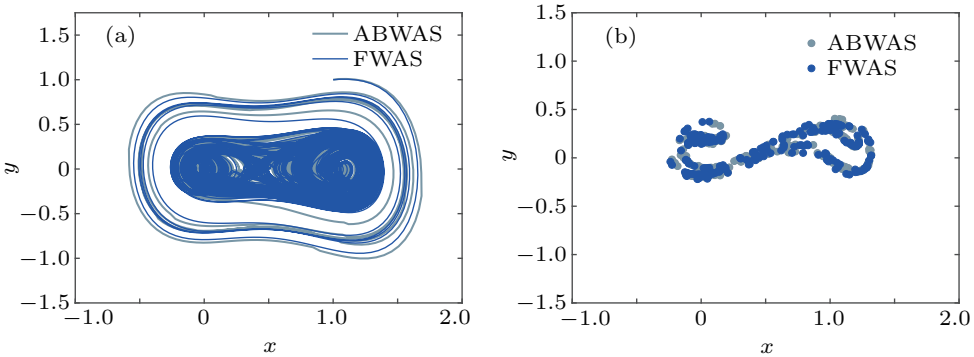


Fig. 2. ABWAS in the case of $q_1 = 1.02$, $q_2 = 0.97$, $\alpha = 0.9$, $\beta = 3$, $\gamma = 2$, $F = 0.11$, $\mu = 0.1$, $\omega = 1$ and FWAS in the case of $q_1 = 1.03$, $q_2 = 0.96$, $\alpha = 0.9$, $\beta = 3$, $\gamma = 2$, $F = 0.11$, $\mu = 0.1$, $\omega = 1$: (a) phase diagram, (b) Poincaré section.

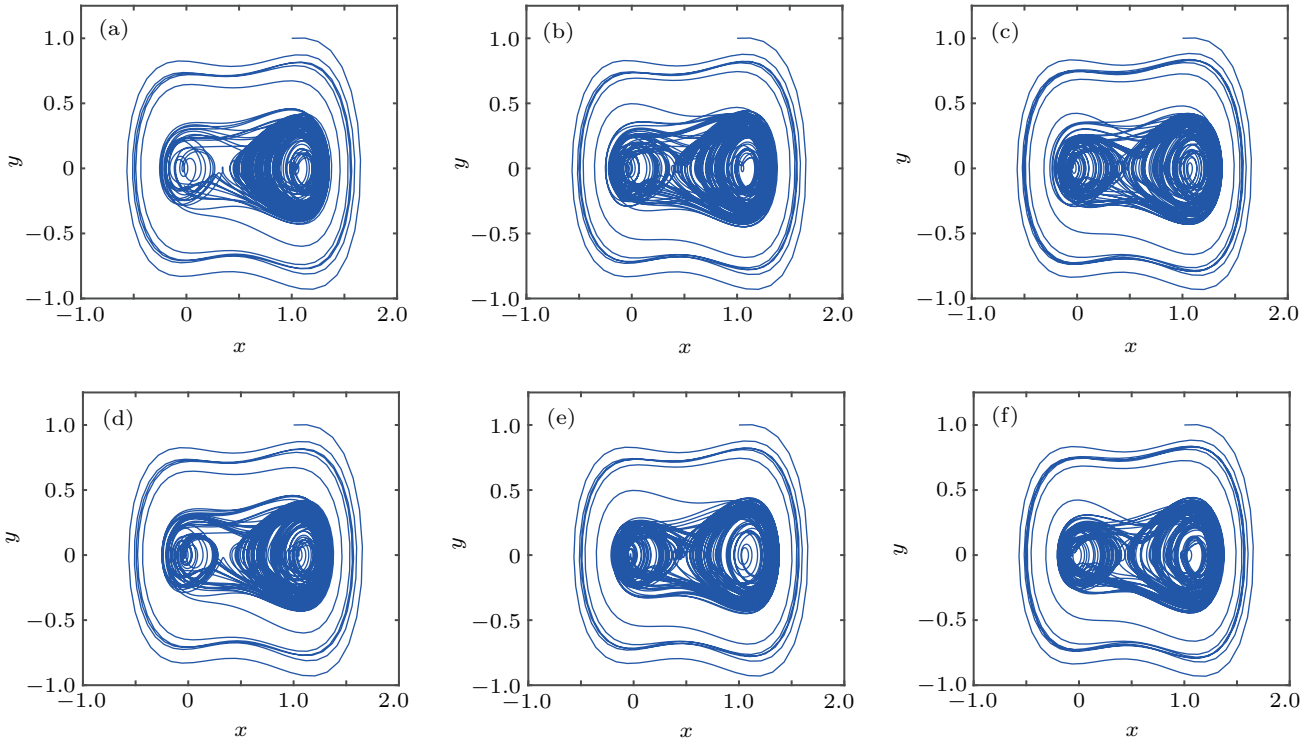


Fig. 3. Phase diagram of FWAS in the case of $q_1 = 1$, $q_2 = 1$, (a) $F = 0.095$; (b) $F = 0.097$; (c) $F = 0.1$. Phase diagram of ABWAS in the case of $q_1 = 1$, $q_2 = 1$, (d) $F = 0.095$; (e) $F = 0.097$; (f) $F = 0.1$.

of F is determined, there are numerical differences between the phase diagrams of the two systems.

3.4. Effects of pulse pressure on ABWAS and FWAS

The following system is obtained with the parameters of $q_1 = 1.02$, $q_2 = 0.97$, $\alpha = 0.9$, $\beta = 3$, $\gamma = 2$, $\mu = 0.1$, $\omega = 1$:

$$\begin{cases} {}_0^{\mathrm{AB}}D_t^{1.02}x = y, \\ {}_0^{\mathrm{AB}}D_t^{0.97}y = F\cos t - 0.1y - 0.9x + 3x^2 - 2x^3. \end{cases} \tag{25}$$

The influence of pulse pressure here mainly refers to the influence of blood pressure on ABWAS. Figure 4 shows the x–F and y–F bifurcation diagrams (system (25)), where F is in the range of $[0.05, 0.2]$. From Fig. 4, we can see that small changes in the pulse pressure F can significantly affect the chaotic state. The system (25) is chaotic in the interval $0.098 \leq F \leq 0.121$ (Figs. 4(a), and 4(b)). The results in Fig. 4 show that when F is greater than 0.121 the system (25) is characterized as stable behavior.

For system (13), we set the same parameters as those of system (25). The results of the numerical simulation are shown in Fig. 5. The system (13) is chaotic in the interval $0.097 \leq F \leq 0.124$ (Fig. 5(a)). In addition, the system (13) is chaotic in the interval $0.095 \leq F \leq 0.123$ (Fig. 5(b)). It is clear that if F is greater than 0.124 (Fig. 5(a)) or 0.123 (Fig. 5(b)) the system (13) is characterized as stable behavior.

It can be seen that when the blood pressure is stable, the blood flow in the cerebral aneurysm is relatively stable. Conversely, the blood flow in the cerebral aneurysm is chaotic, and the cerebral aneurysm is prone to rupture.

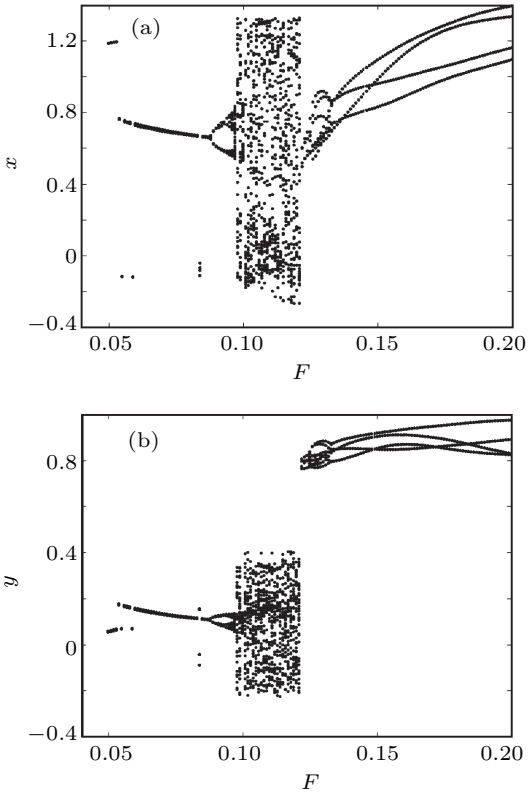


Fig. 4. Bifurcation diagram of system (25) versus pulse pressure F: (a) dependent variable x, (b) dependent variable y.

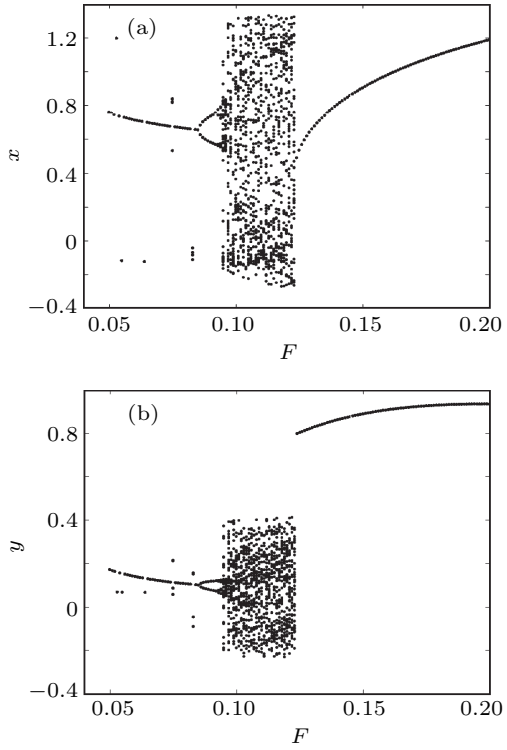


Fig. 5. Bifurcation diagram of system (13) versus pulse pressure F: (a) dependent variable x, (b) dependent variable y.

3.5. Influence of system order q_1 and q_2 on ABWAS and FWAS

The effects of fractional order q_1 and q_2 on system (14) are further discussed for $F = 0.11$ and other parameters remain unchanged. Let the fractional order q_1 varied from 0.9 to 1.044. Figure 6(a) shows the bifurcation diagram (system (14)) of x as a function of q_1. The system (14) is chaotic in the interval $1.008 \leq q_1 \leq 1.044$ (Fig. 6(a)). In Fig. 6(b), we present x–q_2 bifurcation diagram (system (14)), where q_2 is in the range of $[0.9, 0.99]$. Furthermore, the system (14) is chaotic in the interval $0.957 \leq q_2 \leq 0.99$ (Fig. 6(b)).

We can learn from Fig. 6 that the small changes of the order q_1 and q_2 can significantly affect the chaotic state of ABWAS, and the system (14) reaches the chaotic state through the double-cycle bifurcation road.

For system (13), we set the same parameters as those of system (14). The results of the numerical simulation are shown in Fig. 7. The system (13) is chaotic in the intervals $0.981 \leq q_1 \leq 1.027$ (Fig. 7(a)) and $0.94 \leq q_2 \leq 0.977$ (Fig. 7(b)). It is clear that when q_1 is greater than 1.027 (Fig. 7(a)) or q_2 is greater than 0.977 (Fig. 7(b)) the system (13) is characterized as stable behavior.

Compared with that of system (13), the bifurcation diagram of system (14) appears fewer chaotic phenomena.

The system order we select should help us to analyze the dynamic behavior of ABWAS. Further, the chaotic state of ABWAS shows unstable blood flow and rupture of cerebral aneurysms. Therefore, the system order that makes ABWAS in a chaotic state is our focus. It can be seen from Fig. 6 that ABWAS is in chaos when $q_1 = 1.02$ and $q_2 = 0.97$, thus we choose $q_1 = 1.02$ and $q_2 = 0.97$ for research.

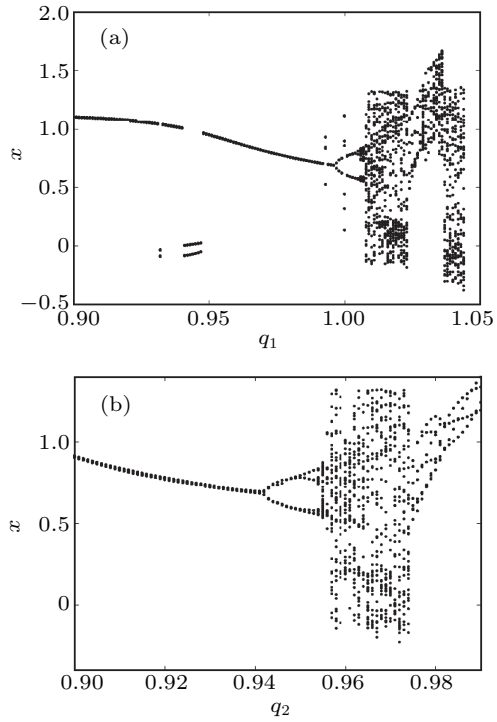


Fig. 6. Bifurcation diagram of ABWAS (14) versus fractional order: (a) q_1, (b) q_2.

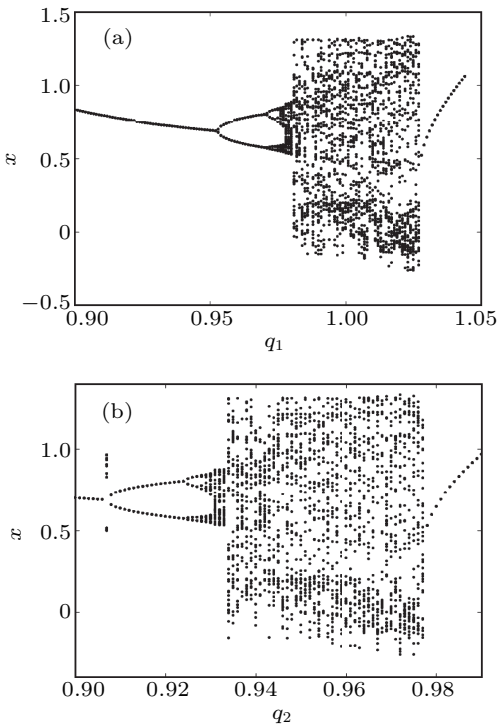


Fig. 7. Bifurcation diagram of system (13) versus fractional order: (a) q_1, (b) q_2.

3.6. Influence of blood flow damping coefficient μ and reciprocal of heart rate ω on ABWAS

In this section, the parameters of system (14) are taken as follows: $\alpha = 0.9$, $\beta = 3$, $\gamma = 2$, $F = 0.11$, $q_1 = 1.02$, $q_2 = 0.97$.

Let the blood flow damping coefficient μ varied from 0 to 1.2. Figure 8(a) shows the μ–x bifurcation diagrams. In Fig. 8(b), we present the ω–x bifurcation diagram (system (14)), where ω is in the range of $[0.01, 2]$.

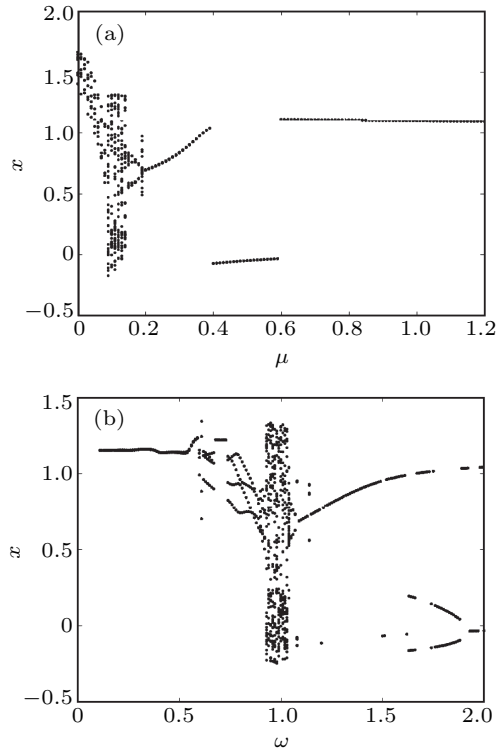


Fig. 8. (a) Bifurcation diagram of system (14) versus coefficient of blood flow damping μ, (b) bifurcation diagram of system (14) versus reciprocal of heart rate ω.

In Fig. 8(a), the velocity of blood flow tends to be stable with the increase of the blood flow damping coefficient. In Ref. [41], the authors proposed that coil embolization can reduce blood flow velocity and induce thrombosis in aneurysms, which is consistent with the numerical simulation results of Fig. 8(a). It can be seen from the bifurcation diagram in Fig. 8(b) that the system (14) gradually changes from chaotic state to steady as the reciprocal of heart rate increases (the heart rate decreases). Liu *et al.* in Ref. [42] explained that drugs that can stabilize or reduce the heart rate have auxiliary effects on the treatment of cerebral aneurysms. This result is consistent with the numerical simulation results of Fig. 8(b). Therefore, it is important for clinical diagnosis to study the effects of blood flow damping coefficient and heart rate derivative on cerebral aneurysms using ABWAS.

4. Control of the chaotic ABWAS and FWAS

The chaotic state of ABWAS is characterized by unstable blood flow. Furthermore, cerebral aneurysms are more likely to rupture in extremely chaotic speed state, which can lead to serious consequences such as headache, vomiting, and disturbance of consciousness. Therefore, the system (14) should be controlled as much as possible to avoid the occurrence of chaos. By designing a suitable controller, the chaotic phenomenon of ABWAS is controlled, where the parameters are set according to the stability conditions of the system.

With the same parameters as those in Section 3, the ABWAS with the initial value condition is obtained as follow:

$$\begin{cases} {}_0^{\mathrm{AB}}D_t^{1.02}x = y, \\ {}_0^{\mathrm{AB}}D_t^{0.97}y = 0.11\cos(t) - 0.1y - 0.9x + 3x^2 - 2x^3, \\ x(0) = 1, \ \ y(0) = 1. \end{cases} \quad (26)$$

Theorem 2 The AB fractional system (26) with initial conditions is not stable.

Proof According to Theorem 1, we have

$$\begin{aligned} P(x,y) &= xy + y\left(0.11\cos(t) - 0.1y - 0.9x + 3x^2 - 2x^3\right) \\ &\le 0.1xy + 0.11y - 0.1y^2 + 3x^2y - 2x^3y \\ &\le 0.05x^2 + 0.05y^2 + 0.11y - 0.1y^2 \\ &\quad + 1.5x^4 + 1.5y^2 - 2x^3y \\ &= 0.05x^2 + 0.11y + 1.5x^4 + 1.45y^2 - 2x^3y. \end{aligned} \quad (27)$$

Since the value of the function $P(x,y)$ cannot be estimated, the stability of the system (26) becomes difficult to determine. However, according to the simulation results of Fig. 1, we can conclude that ABWAS (26) with initial conditions is not stable. Proof is completed.

In the quest to stabilize the system (26), a controller system is introduced as follow:

$$\begin{cases} {}_0^{\mathrm{AB}}D_t^{1.02}x = y - k_1x, \\ {}_0^{\mathrm{AB}}D_t^{0.97}y = 0.11\cos(t) - 0.1y - 0.9x + 3x^2 \\ \qquad\qquad - 2x^3 - k_2\left(y - \dfrac{11}{100k_2}\right), \\ x(0) = 1, \ \ y(0) = 1. \end{cases} \quad (28)$$

Theorem 3 The controller-controlled AB fractional system (28) is stable if $k_1 \ge 0.105$, $k_2 \ge 0.005$, and $y \le 0$.

Proof According to Theorem 1, the function $P(x,y)$ is obtained as follow:

$$\begin{aligned} P(x,y) &= x(y - k_1x) + y\big(0.11\cos(t) - 0.1y - 0.9x \\ &\quad + 3x^2 - 2x^3 - k_2(y - \frac{11}{100k_2})\big) \\ &= xy - k_1x^2 + 0.11y\cos t - 0.1y^2 - 0.9xy \\ &\quad + 3x^2y - 2x^3y - k_2y^2 + 0.11y \\ &\quad y \le 0, \ 0.11\cos(t)y + 0.11y \le 0 \\ &\le 0.1xy - k_1x^2 - 0.1y^2 + 3x^2y - 2x^3y - k_2y^2 \\ &= 0.1xy - k_1x^2 - 0.1y^2 \\ &\quad + xy(3x - 2x^2 - 0.11) + 0.11xy - k_2y^2 \\ &\quad 0.0376 \le x \le 1.4624, \ 3x - 2x^2 - 0.11 \ge 0 \\ &\le 0.1xy - k_1x^2 - 0.1y^2 + 0.11xy - k_2y^2 \\ &\le 0.105x^2 + 0.105y^2 - k_1x^2 - 0.1y^2 - k_2y^2 \end{aligned}$$

$$= (0.105 - k_1)x^2 + (0.005 - k_2)y^2. \quad (29)$$

The function $P(x,y) \leq 0$ for $k_1 \geq 0.105$ and $k_2 \geq 0.005$. Therefore, according to Theorem 1, the controller-controlled AB fractional system (28) is stable. Theorem 3 is verified.

With $k_1 = 0.3$ and $k_2 = 1.4$, the simulation results of system (28) are shown in Fig. 9. From the results of the Poincaré section and phase diagram in Fig. 9, it can be seen that the controlled ABWAS (28) is quickly limited to small-scale range periodic fluctuations and amplitude.

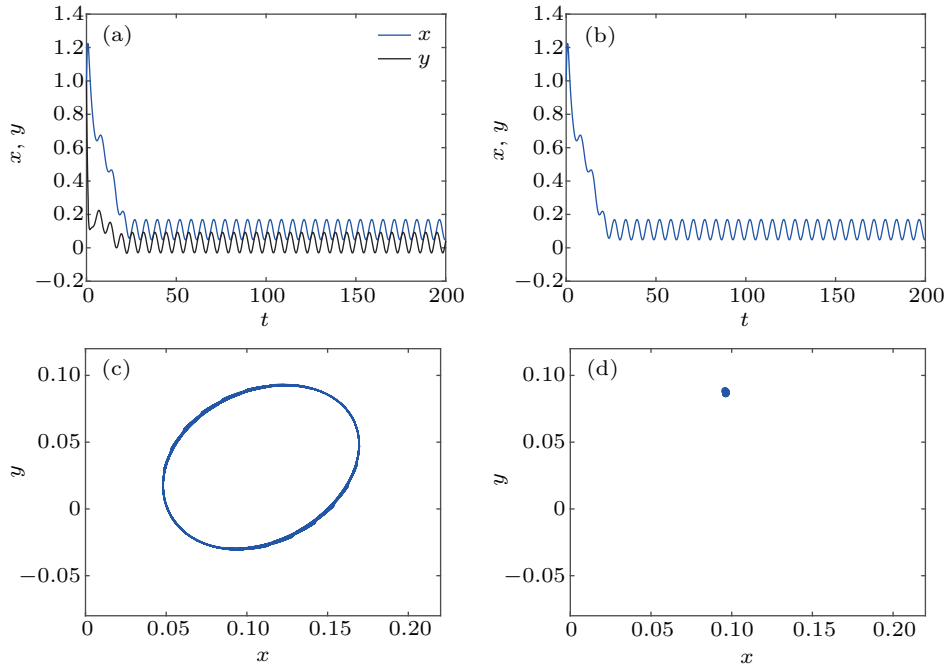


Fig. 9. The control of ABWAS with controller (28): (a) curves of x–t and y–t, (b) time course, (c) phase diagram, (d) Poincaré section.

The bifurcation diagrams of the controller-controlled ABWAS (28) with the fractional order q_1 and q_2 are presented in Fig. 10. For the Caputo fractional Willis aneurysm system (13), we design the same controller as system (28). Furthermore, we set the same parameters as those of system (28) and $k_1 = 0.3$, $k_2 = 1.4$. The results of the numerical simulation are shown in Fig. 10. Under the influence of q_1, the steady blood flow velocity of the controller-controlled ABWAS varies from 0.1024 to 0.0858 and the steady blood flow velocity of the controller-controlled FWAS varies from 0.1025 to 0.0906 (Fig. 10(a)). In addition, when q_2 is in the range of 0.9 to 0,99, the maximum steady blood flow velocity is 0.0966 for the controller-controlled ABWAS and equals to 0.0994 for the controller-controlled FWAS. Furthermore, the minimum steady blood flow velocity is 0.0955 and 0.0973 for the controller-controlled ABWAS and the controller-controlled FWAS, respectively. From Fig. 10, we can observe that after introducing the controller, the chaotic interval of system (28) also becomes a stable interval.

Figures 10 present the comparative study between system (28) and the Caputo fractional Willis aneurysm system with same controller. From Fig. 10, we can see that the blood flow velocity (x) of system (28) changes in a smaller steady value compared to the Caputo fractional Willis aneurysm system with the same controller.

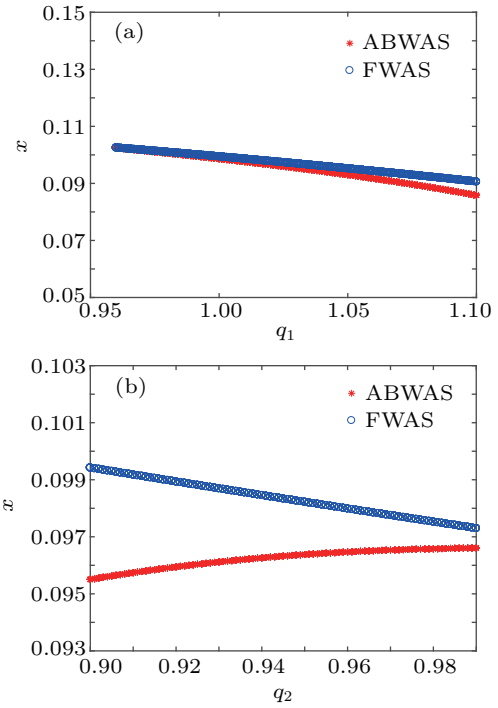


Fig. 10. Bifurcation diagrams of system (28) with controller and system (13) with controller versus fractional order: (a) q_1, (b) q_2.

5. Conclusion

In view of the fact that the Atangana–Baleanu fractional derivative can better describe the complex dynamics of blood flow, we establish a Willis aneurysm system based on the Atangana–Baleanu fractional derivative. The research results show that ABWAS is chaotic under the certain parameter values. Comparing to the bifurcation diagrams of order and pulse pressure of FWAS, the bifurcation diagrams of ABWAS show that less chaos occurs in the same ranges of order and pulse pressure. Therefore, we conclude that the order and pulse pressure have a significant effect on ABWAS.

With the increase of blood flow damping coefficient μ or reciprocal heart rate ω, the system tends to be stable. These results accord with the clinical treatment of cerebral aneurysms using the method of drugs or coils embolization. Therefore, the study of blood flow damping coefficient and reciprocal heart rate has certain significance for clinical diagnosis and treatment of cerebral aneurysms.

By designing a suitable controller based on the stability theorem, the blood flow velocity of the ABWAS can be stabilized in a short time. In addition, compared with the bifurcation diagrams of the controller-controlled Caputo fractional order Willis aneurysm system, under the same parameters, the blood flow velocity of the controller-controlled ABWAS changes within a smaller numerical interval. Therefore, the control effect on the ABWAS is better. This paper provides a theoretical basis for the study on the chaotic control and treatment of brain aneurysms.

References

[1] Ji Q B, Zhou Y, Yang Z Q and Meng X Y 2015 *Chin. Phys. Lett.* **32** 050501
[2] Wang X Y, Wang Y, Wang S W, Zhang Y Q and Wu X J 2018 *Chin. Phys. B* **27** 110502
[3] Zhang R, Peng M, Zhang Z D and Bi Q S 2018 *Chin. Phys. B* **27** 110501
[4] Sadasivan C, Fiorella D J, Woo H H and Lieber B B 2013 *Ann. Biomed. Eng.* **41** 13471365
[5] Austin G 1971 *Math. Biosci.* **11** 163172
[6] Liu T Y and Wan S D 1989 *J. Biomath.* **1** 2128 (in Chinese)
[7] Liu T Y and Li C X 1990 *J. Yunnan Inst. Technol.* **4** 0108 (in Chinese)
[8] Cao J D and Liu T Y 1993 *J. Biomath.* **2** 0916 (in Chinese)
[9] Yang C H and Zhu S M 2003 *Acta Sci. Nat. Univ. Sunyatseni* **42** 0103 (in Chinese)
[10] Feng C H 1998 *J. Biomath.* **13** 6164 (in Chinese)
[11] Nieto J J and Torres A 2000 *Nonlinear Anal.* **40** 513521
[12] Li Y M and Yu S 2008 *J. Biomath.* **23** 235238 (in Chinese)
[13] Peng S H, Li D H, Su Z and Li H D 2010 *Comput. Eng. Appl.* **46** 245248 (in Chinese)
[14] Sun M H, Xiao J and Dong H L 2016 *Highlights of Sciencepaper Online* **9** 640 (in Chinese)
[15] Gao F, Li T, Tong H Q and Ou Z L 2016 *Acta Phys.Sin.* **65** 5262 (in Chinese)
[16] Atangana A 2015 *Derivative with a new parameter: Theory, methods and applications* (New York: Academic Press) pp. 73–150
[17] Sheikh N A, Ali F, Khan I and Saqib M 2018 *Neural Comput. Appl.* **30** 18651875
[18] Caputo M and Fabrizio M 2015 *Progr. Fract. Differ. Appl.* **1** 7385
[19] Saqib M, Ali F, Khan I, Sheikh N A, Jan S A A and Samiulhaq 2018 *Alexandria Eng. J.* **57** 18491858
[20] Atangana A and Gómez-Aguilar J F 2017 *Chaos, Solitons Fractals* **102** 285294
[21] Atangana A and Gómez-Aguilar J F 2017 *Physica A* **476** 0114
[22] Atangana A and Baleanu D 2016 *Therm. Sci.* **20**
[23] Gómez-Aguilar J F, Escobar-Jiménez R F, Lǿpez-Lǿpez M G and Alvarado-Martínez V M 2016 *J. Electromagn. Waves. Appl.* **30** 19371952
[24] Bas E and Ozarslan R 2018 *Chaos, Solitons Fractals* **116** 121125
[25] Owolabi K M 2018 *Eur. Phys. J. Plus* **133** 15
[26] Coronel-Escamilla A, Gómez-Aguilar J, Baleanu D, Cérdova-Fraga T, Escobar-Jimónez R, Olivares-Peregrino V and Qurashi M 2017 *Entropy* **19** 55
[27] Gómez-Aguilar J, Morales-Delgado V, Taneco-Hernández M, Baleanu D, Escobar-Jiménez R and Al Qurashi M 2016 *Entropy* **18** 402
[28] Gómez-Aguilar J F, Atangana A and Morales-Delgado V F 2017 *Int. J. Circuit Theory Appl.* **45** 15141533
[29] Kashif A A, Mukkarum H and Mirza M B 2017 *Eur. Phys. J. Plus* **132** 439
[30] Sheikh N A, Ali F, Khan I, Gohar M and Saqib M 2017 *Eur. Phys. J. Plus* **132** 540
[31] Asjad M I, Miraj F and Khan I 2018 *Eur. Phys. J. Plus* **133** 224
[32] Sheikh N A, Ali F, Saqib M, Khan I, Jan S A A, Alshomrani A S and Alghamdi M S 2017 *Results Phys.* **7** 789800
[33] Alqahtani R T 2016 *J. Nonlinear. Sci. Appl.* **9** 36473654
[34] Atangana A 2017 *Fractional operators with constant and variable order with application to geo-hydrology* (New York: Academic Press) pp. 52–130
[35] Atangana A and Koca I 2016 *Chaos, Solitons Fractals* **89** 447454
[36] Omar A A and Al-Smadi M 2018 *Chaos, Solitons Fractals* **117** 161167
[37] Zhu K Q 2009 *Mech.Pract.* **31** 104 (in Chinese)
[38] Lu K Q and Liu J X 2009 *Physics* **38** 453 (in Chinese)
[39] Saif U, Muhammad A K and Muhammad F 2018 *Eur. Phys. J. Plus* **133** 313
[40] Alkahtani B S T 2016 *Chaos, Solitons Fractals* **89** 547551
[41] Wu Y F, Shen J, Huang Q H, Xiang J P, Meng H and Lu J M 2012 *Acad. J. Second Mil. Med. Univ.* **33** 195199 (in Chinese)
[42] Liu X and Wen C 2018 *Med. Philos.* **39** 3336 (in Chinese)